Journal of Luminescence 227 (2020) 117549

Contents lists available at ScienceDirect

Journal of Luminescence

journal homepage: http://www.elsevier.com/locate/jlumin

Luminescence enhancement by water replacement in Eu@COK-16 metal organic framework

Ivan G.N. Silva, Danilo Mustafa *

Instituto de Física da Universidade de São Paulo, 05508-090, São Paulo, SP, Brazil

A B S T R A C T

Metal Organic Framework (MOF) exhibits interesting structural properties especially considering their ion exchange capacity. Eu@COK-16 have been shown to present a small emission quantum efficiency due to the high amount of water molecules in their structure. This report presents a series of Eu@COK-16 with luminescence enhancement due to the replacement of the suppressor molecules by impregnation with organic ligands such as acetylacetonate (ACAC), butyl sulfoxide (Butyl) and dimethyl sulfoxide (DMSO). Spectroscopic investigation, *i.e.* excitation/emission spectra and lifetimes of the excited states, shows an increase in the quantum efficiency owing to the successful elimination of water molecules from the first coordination sphere of the Eu^{3+} ions.

1. Introduction

Hybrid luminescent metal organic framework has been highlighted in the last decade as a promising material thanks to the presence of luminescent centers in a such pore system, offering the ability to accommodate guest molecules close to the luminescent species. Organic ligands in coordination compound as Metal Organic Frameworks (MOFs) can act as an antenna, absorbing and transferring efficiently the energy to the rare earth ions as an alternative to overcome the rare earth reduced luminescence due to their low intrinsic absorptivity [1–4]. The interest in the photoluminescence study of those molecular systems based on trivalent (RE^{3+}) rare earths has increased significantly since the application of organic ligands as the building blocks of the three-dimensional MOF structure and luminescence sensitizers leading to the development of light conversion molecular devices (LCMDs) [5,6]. As an example, the Eu@COK-16: HPA@$Cu_3(BTC)_2{\cdot}3(H_2O)$ with Eu^{3+} (HPA: phosphotungstic acid, BTC: trimesic acid or 1,3,4-benzenetricarboxylic acid) was demonstrate to be a new concept of luminescent host–guest materials [7]. In this system, the antenna molecules are part of the framework structures and, however the $PW_{12}O_{40}^{3-}$ ions partly occupy one of the three types of pores presented by this structure, a considerable portion of the pore volume in this host sensitized luminescent mesoporous material remains available for adsorption of additional sensitizing molecules. Despite the promising suitability of those materials for applications as persistent phosphors [8], structural probes [9,10], luminescent markers [11,12], display panels [13,14], fluoroimmunoassay [15,16], *etc.*, their luminescence still tailored by the presence of water molecules in the first coordination sphere of the trivalent rare earth (RE). This suppressors molecules provide a non-radiative depopulation pathway of the RE^{3+} excited state [17].

This report describes a study on the luminescence effects of replacing the coordinated water of Eu^{3+} hosted in the framework of Eu@COK-16 (containing three hydration waters) by acetylacetonate (ACAC), butyl sulfoxide (Butyl) e dimethyl sulfoxide (DMSO) coordination complexes. The phenomenological intensity parameters ($\Omega_{2,4}$), the radioactive (A_{rad}), non-radioactive (A_{nrad}) and total (A_{tot}) spontaneous emission rates, main emitting state lifetime $^5D_0$ (τ) and quantum efficiency (η) of Eu^{3+} in those systems were obtained based on the on the Judd-Ofelt theory. Overall, according to this spectroscopic investigation, the impregnation of Eu@COK-16 with the organic ligands leads to an enhancement in the luminescence revealed by the increase in the quantum efficiency (η) of the rare earth activator.

2. Experimental section

The $EuCl_3{\cdot}6(H_2O)$ salt was obtained by addition of concentrated hydrochloric acid to an aqueous suspension of Eu_2O_3 (Cstarm, 99.99 mol %). Trimesic acid (H_3(BTC) – Fluka, 97 mol%), phosphotungstic acid (HPA - Fluka, 97 mol%), $Cu(NO_3)_2{\cdot}3(H_2O)$ (Synth, 99 mol%), absolute ethanol (VWR) were used without further purification. The coordination complexes (Fig. 1) dimethyl sulfoxide (DMSO, 99 mol%), acetylacetone (ACAC, 99 mol%) and butyl sulfoxide (Butyl, 96 mol%) were purchased from Sigma Aldrich. The Eu@COK-16 synthesis was performed following the description of Mustafa *et al.* [7].

Powder X-ray diffraction measurements were performed in a Higaku Miniflex II with a CuKa source and a Bragg angle 2θ ranged from 3 to

* Corresponding author.
E-mail address: dmustafa@if.usp.br (D. Mustafa).

https://doi.org/10.1016/j.jlumin.2020.117549
Received 25 March 2020; Received in revised form 29 June 2020; Accepted 22 July 2020
Available online 23 July 2020

60°. Scanning Electron Microscope (SEM) measurements were obtained using a JEOL JSM-740 1F (Field Emission Scanning Electron Microscope). The emission and excitation spectra of the samples were obtained using a Fluorolog 3 (Horiba) in a front face mode (22.5°) with a 450W Xenon lamp as excitation source. The same setup provides lifetime measurements (micro/millisecond scale) by monitoring the hypersensitive (Eu^{3+}) $^5D_0 \rightarrow {}^7F_2$ transition while using a pulsed xenon lamp able to excite at the higher intensity ligand band.

3. Results and discussion

Vacuum dried COK-16 [18] crystals were suspended in a 1:1 water: ethanol 1:1 $EuCl_3$/HPA@$Cu_3(BTC)_2{\cdot}3(H_2O)$ solution. After reaction for 7 days, the success of the ion exchange can be easily checked by both the Cu^{2+} ions released into the solution and the appearance of the characteristic hypersensitive transition Eu^{3+}-$^5D_0 \rightarrow {}^7F_2$ (618 nm) of Eu^{3+} in the MOF's emission spectrum [7,18]. Afterwards the crystals were washed twice with absolute ethanol to remove non-coordinated Eu^{3+} and Cu^{2+} and dried under reduced pressure at room temperature, resulting in a hybrid luminescent Eu@COK-16 [7].

According to Mustafa et al. [7], the Eu^{3+} in the Eu@COK-16 obtained by replacing "extra-framework" Cu^{2+} ions occupy a non-centrosymmetric 9-coordinate sites on the surface of $PW_{12}O_{40}^{3-}$ ions, responsible for the cation exchange property of the Eu@COK-16 [7,18]. In addition to the 4 Oxygen atoms of $PW_{12}O_{40}^{3-}$, the coordination of the Eu is complete by 4 water molecules and a simple coordination with the carboxylic group of the additional BTC molecules present in the pores. As a result, a quadratic anti-prism is formed by oxygen from HPA and water, which is covered on one square face by oxygen atoms from the extra-framework BTC molecules. The symmetry of this coordination is consistent with symmetry C4 in the first sphere of coordination of the Eu^{3+}. As known, the occurrence of water molecules in the first coordination sphere of trivalent rare earth ions provide a non-radiative depopulation pathway for the RE^{3+} excited state, responsible for the luminescence quenching of the emission center [2,19–21].

3.1. Replacement of coordination waters

Since the appearance of those non-radiative centers associated to the Eu^{3+}-coordinated water molecules, a series of experiments were performed to replace the water by coordination complexes to overcome the suppression of its luminescence, likely improving the Eu@COK-16 quantum efficiency.

The MOF crystals were soaked with acetylacetonate (ACAC), butyl sulfoxide (Butyl) and dimethyl sulfoxide (DMSO). In order to accelerate the ligand exchange reaction and eliminate excess solvent/binder, the system was heated to 393 K for 72h. The procedure promotes the exchange of coordination water molecules for those coordination chromophores (Eu@COK-16+coordnation complexes).

Fig. 2 shows the X-ray powder diffraction patterns (PXRD) for the COK-16, the Eu@COK-16 and after its impregnation with DMSO, Butyl, ACAC1 and ACAC2 (ACAC2 = 10 ACAC1). The presence of the characteristic peaks of COK-16 in the diffraction patterns and the absence of changes in their positions suggest the preservation of the $Cu_3(BTC)_2$ structure in the samples. The decrease in intensities and the widening of the peaks observed specially for samples impregnated with ACAC1 and ACAC2 suggest a structural degradation of the Eu@COK-16. Besides, the competition between Cu^{2+} and Eu^{3+} for the coordination complexes and the possibility of a second phase formation can also contribute to the changes in the diffractions peaks observed in Fig. 2.

SEM images presented in Fig. 3 show the presence of crystals with the expected octahedral shape characteristic of the $Cu_3(BTC)_2$ MOFs. In the case of the COK-16 sample, the Eu@COK-16 and the samples impregnated with DMSO and Butyl it is clear the preservation of the structure, in accordance to the PXRD measurements. On the other hand, for the samples subject to ACAC1 and ACAC2, besides the indication of a second morphology, the particles start to degrade as can been seen by the formation of holes in the octahedral crystals once again corroborated by the X-ray diffraction results. In this case, due to the high affinity of these coordination complexes with the Eu^{3+}, not only the complexes can replace the water molecules but they can also remove the Eu^{3+} from the structure. In addition, the ACAC is similarly able to coordinate structural Cu^{2+} in the Eu@COK-16. These two effects can be responsible for the crystals disruption demonstrate by the SEM images in Fig. 3 (e and f).

3.2. Luminescent proprieties

Fig. 4 (left) shows the excitation spectra monitoring the

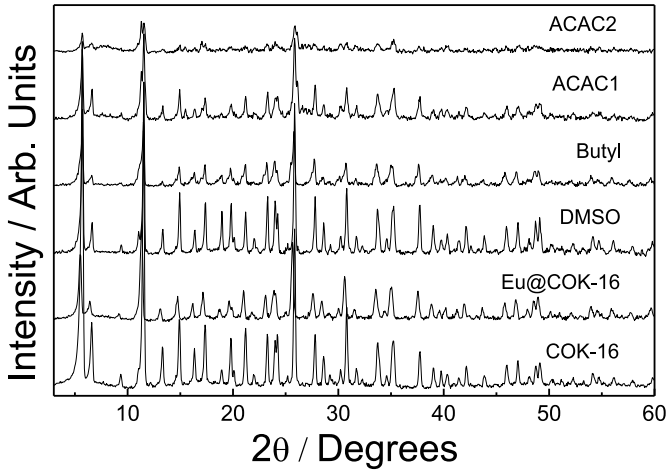

Fig. 2. X-ray powder diffraction patterns of COK-16, Eu@COK-16 and after the impregnation with the coordination complexes.

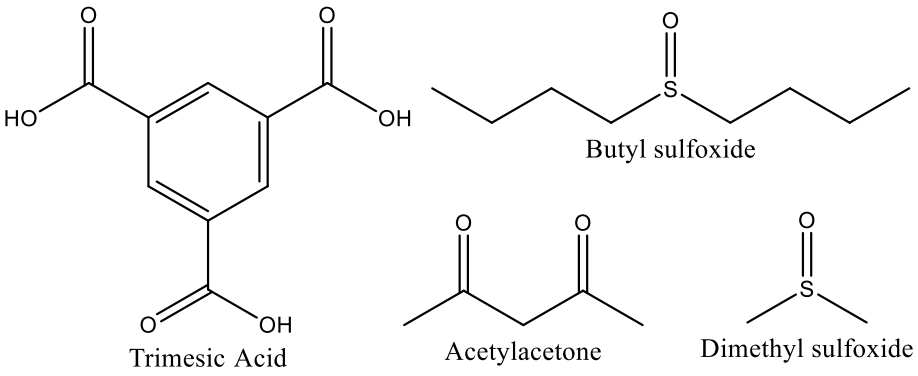

Fig. 1. Structures of the organic ligands.

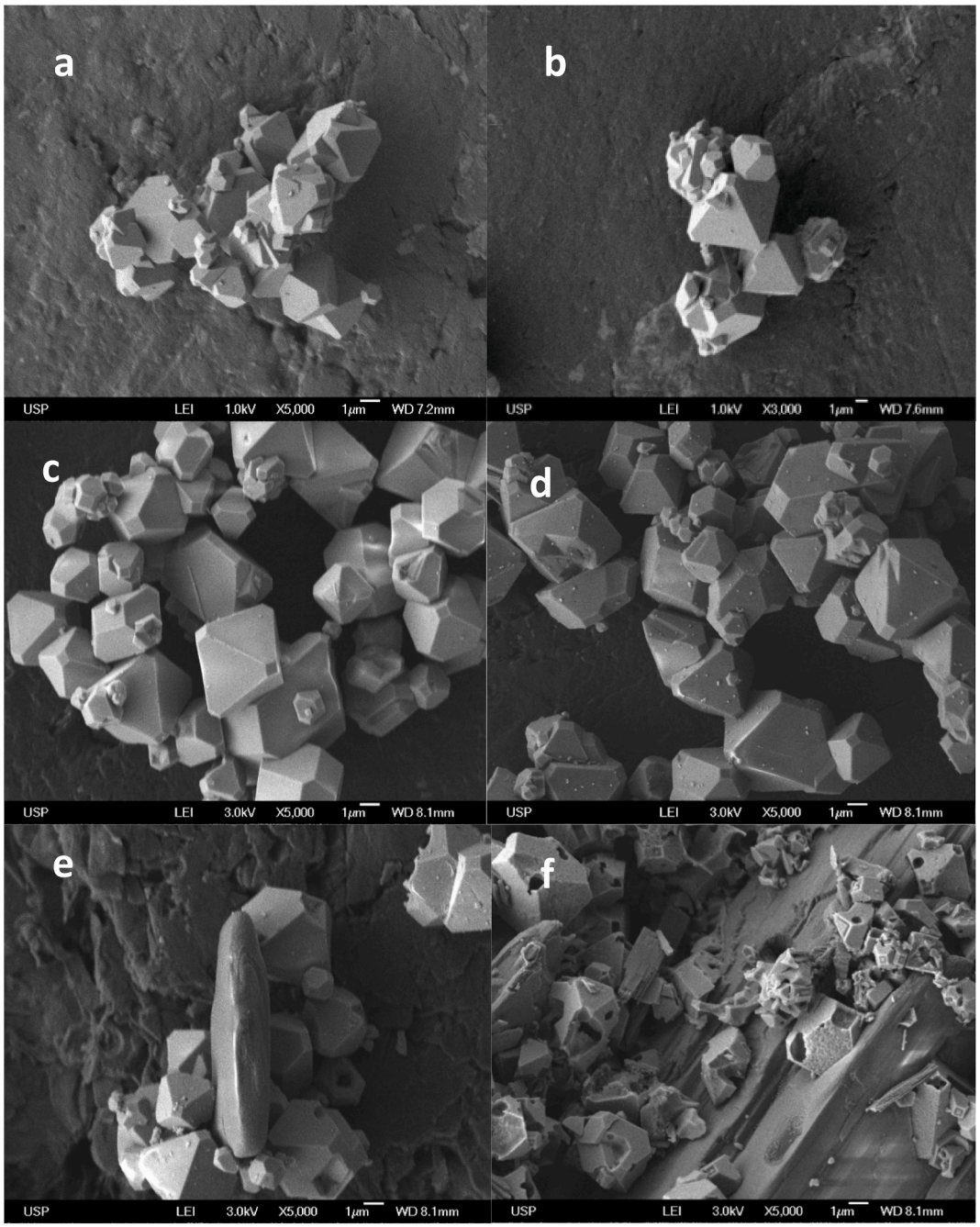

Fig. 3. Scanning Electron Microscopy - SEM images of COK-16 samples. a) COK-16. b) 10Eu:1COK-16 after ion exchange for 7 days (Eu@COK-16) c), d), e) and f) impregnated with DMSO, Butyl, ACAC1 and ACAC2, respectively.

hypersensitive transition (Eu^{3+}) $^5D_0 \rightarrow {}^7F_2$ (611 nm) for the Eu@COK-16 and the samples impregnated by DMSO, Butyl and ACAC1 (lower concentration) recorded from 200 to 580 nm at 300 K. The broad bands centred at 260 and 295 nm, present in all spectra, is owing to the HPA Ligand to Metal Charge Transfer band, LMCT, (O→W) and BTC ligand $S_0 \rightarrow S_n$ transition, respectively. On the other hand, the narrower lower intensity bands between 350 and 550 nm are related to the main energy levels of the Eu^{3+}.

The overall spectral profile observed (bands assigned to the BTC ligand and HPA structural anchor) indicates that the basic structure of Eu@COK-16 is preserved after the water substitution [22,23], as shown by X-ray diffraction patterns.

Except for the sample impregnated with Butyl, which presents the smallest variation in its spectral profile, it is clear the change in the relative intensities of the characteristic Eu^{3+} transitions compared to the structural ligand band (BTC) and the low relative intensity of the LMCT band (O→W) at 260 nm. This behaviour can be assigned to modifications on the short distances coordination around the Eu^{3+} due to the water/ligands substitution [1,24,25].

The emission spectra shown in Fig. 4 (right) were recorded at 300 K from 400 to 750 nm with excitation in the BTC ligand band at 295 nm. All the spectra exhibit the characteristic narrow emission lines arising from the $^5D_0 \rightarrow {}^7F_J$ transitions (J: 0–4) of Eu^{3+}. The $^5D_0 \rightarrow {}^7F_0$ transition presents only one emission band indicating that the Eu^{3+} ion occupies one symmetry site. The small widening of the band presented by the impregnated samples indicates the formation of a set of similar, but slightly different, symmetry centers, compared to the Eu@COK-16.

In all the spectra is possible to observe a higher intensities $^5D_0 \rightarrow {}^7F_2$

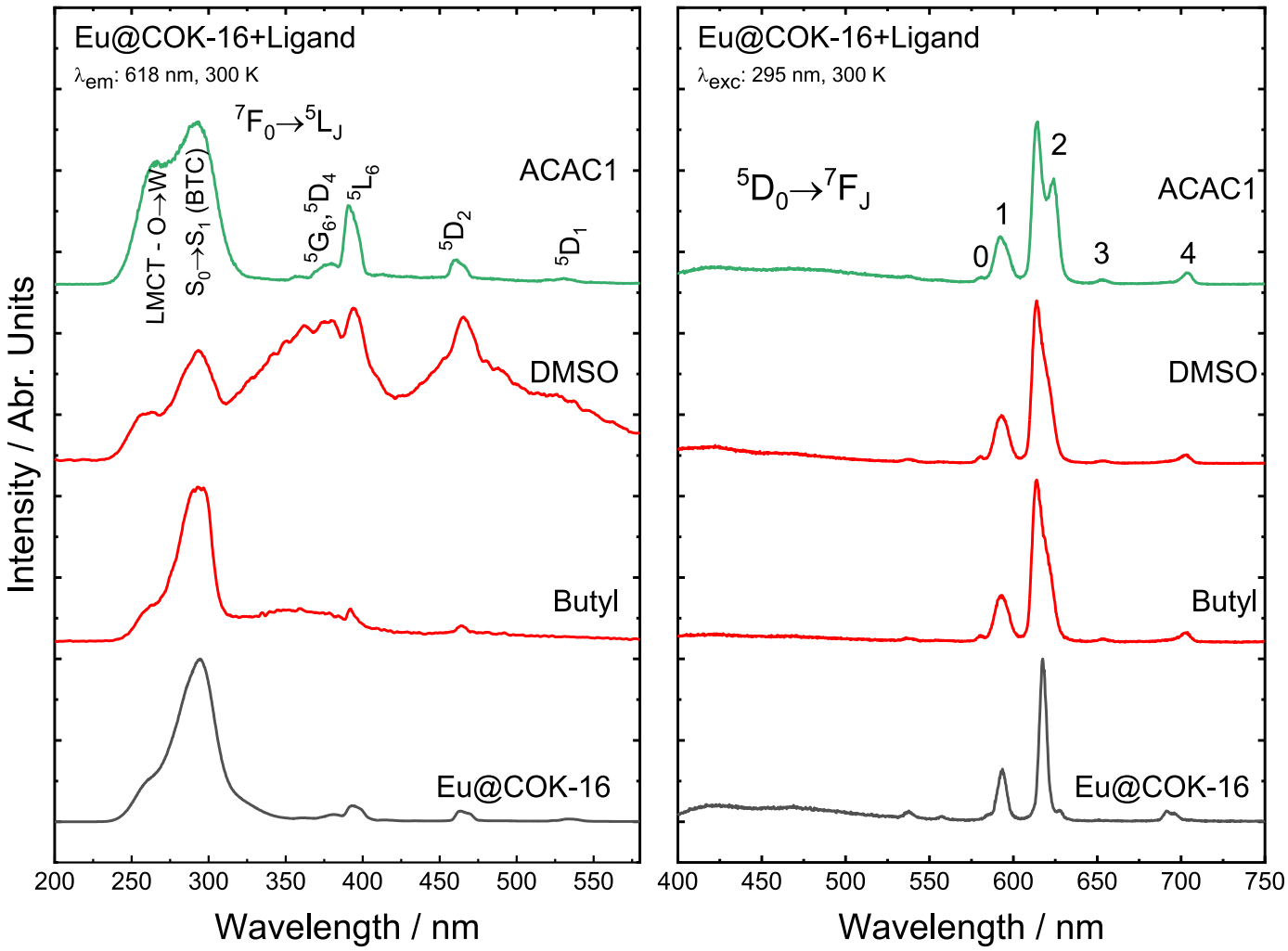

Fig. 4. Excitation (left) and emission (right) spectra of Eu@COK-16 and impregnated with DMSO, Butyl, ACAC1.

hypersensitive transition (characteristic for non-centrosymmetric point groups and allowed by forced electric dipole mechanism) compared to the $^5D_0 \rightarrow {}^7F_1$ transition (allowed by magnetic dipole mechanism), indicating the absence of a centrosymmetric character. The $^5D_0 \rightarrow {}^7F_2$ for the impregnated samples also show a broadening behavior compared to the water molecules coordinated MOFs. The Eu@COK-16+ACAC shows an extra peak in the $^5D_0 \rightarrow {}^7F_2$ transition. This phenomenon could be explained assuming two hypothesis: first, in the case of absence of major structural changes it behavior could be consistent with the exchange of water for the ACAC coordination complex; second possibility is that the split of the $^5D_0 \rightarrow {}^7F_2$ transition indicates the presence of a second phase, probably associated with the formation of the $Eu(ACAC)_3{\cdot}3(H_2O)$ complex after the partial erosion of the Eu@COK-16 crystals.

Using the relative intensities of the emission spectra it is possible to obtain the radiative rates ($A_{0\rightarrow J}$) for the $^5D_0 \rightarrow {}^7F_J$ transitions by Eq. (1):

$$A_{0\rightarrow J} = \frac{\sigma_{0\rightarrow 1}}{S_{0\rightarrow 1}} \frac{S_{0\rightarrow J}}{S_{0\rightarrow J}} A_{0\rightarrow 1} \quad (1)$$

where $\sigma_{0\rightarrow 1}$ and $\sigma_{0\rightarrow J}$ correspond to the energy barycenters of the $^5D_0 \rightarrow {}^7F_1$, taken as the reference due to its pure magnetic dipole character, and $^5D_0 \rightarrow {}^7F_J$ transitions, respectively. The $S_{0\rightarrow 1}$ and $S_{0\rightarrow J}$ are the specific band emission area of the corresponding to the $^5D_0 \rightarrow {}^7F_1$ and $^5D_0 \rightarrow {}^7F_J$ transitions, respectively. Since the magnetic dipole $^5D_0 \rightarrow {}^7F_1$ transition is almost insensitive to alteration in chemical environment around the Eu^{3+} ion the $A_{0\rightarrow 1}$ rate can be used as an effective internal standard to determine the $A_{0\rightarrow J}$ coefficients for Eu^{3+} compounds [26–28].

The lifetime (τ) of the Eu^{3+}-containing systems materials were obtained from the luminescence decay curve using a monoexponential decay. The emission quantum efficiency (η) of the $^5D_0$ emitting level can be determined according to Eq. (2):

$$\eta = \frac{A_{rad}}{A_{rad} + A_{nrad}} \quad (2)$$

where the total decay rate, $A_{tot} = 1/\tau = A_{rad} + A_{nrad}$ and the $A_{rad} = \Sigma_J A_{0\rightarrow J}$. The A_{rad} and A_{nrad} are the radiative and non-radiative rates, respectively. Table 1 shows the experimental values of the radiative (A_{rad}) and non-radiative (A_{nrad}) rates, and emission quantum efficiency

Table 1
Experimental intensity parameters ($\Omega_{2;4}$), radioactive (A_{rad}), non-radioactive (A_{nrad}) and total (A_{tot}) spontaneous emission rates, main emitting state lifetime $^5D_0$ (τ) and quantum efficiency (η) for Eu@COK-16 samples before and after impregnated with the coordination complexes.

	Ω_2 (10^{-20} cm^2)	Ω_4 (10^{-20} cm^2)	A_{rad} (s^{-1})	A_{nrad} (s^{-1})	A_{tot} (s^{-1})	τ (ms)	η (%)
Eu@COK-16	4.5	1.1	202	7490	7692	0.14	2.6
DMSO	6.0	0.8	240	5920	6160	0.19	3.9
BUTYL	6.0	1.0	246	5914	6160	0.11	4.0
ACAC1	7.0	0.9	269	4959	5228	0.16	5.1

(η).

The transitions $^5D_0 \rightarrow {}^7F_2$ and $^5D_0 \rightarrow {}^7F_4$ can be used to estimate the experimental intensity parameters (Ω_λ, $\lambda = 2$ and 4). The Ω_6 intensity parameter is not included in this study since the $^5D_0 \rightarrow {}^7F_6$ transition was not observed in these materials. The coefficient of spontaneous emission, A, is given by Eq. (3):

$$A_{0\rightarrow J} = \frac{4e^4\omega^3}{3hc^3} x \sum_\lambda \Omega_\lambda \langle {}^7F||U^{(\lambda)}||{}^5D_o\rangle^2 \quad (3)$$

where, $\chi = n\,(n+2)^2/9$ is the Lorentz local field correction and n is the refraction index of the medium (1.5 for these materials). The square reduced matrix elements $\langle {}^7F_J||U^{(\lambda)}||{}^5D_J\rangle^2$ are 0.0032 and 0.0023 calculated for J = 2 and 4, respectively [2,29].

The Ω_λ parameters depends on several factors: local geometry, bonding atom ability to donate electrons and polarizabilities, especially in the first coordination sphere of metal ion. However, according to Judd-Ofelt theory, the Ω_2 values are by far the most sensitive to angular changes in the chemical environment around the Eu^{3+} ion, and it tends rapidly to decrease as the local symmetry tends to higher symmetries or an inversion centre. On the other hand, Ω_4 and Ω_6 are by far the most sensitive to the ligating atoms – metal ion distances and electron donor-acceptor effect [1,2,4,30].

Table 1 shows the values for the experimental intensity parameters calculated for the samples impregnated with the coordination ligands. The increase in the Ω_2 parameter indicates a reduction in the centro-symmetric character induced by the coordinated ligands, *i.e.* a less symmetrical chemical environment around the Eu^{3+} (total or partial elimination of three water molecules). On the other hand, the Ω_4 parameter shows no change, probably owing to the coordinating atom for all systems is oxygen [1,2,20].

According to the results for η, there is an improvement in the quantum yield of the impregnated samples compared to the as prepared Eu@COK-16. This effect can be explained by the replacement of the luminescence suppression centers (represented by the water molecules that completed the Eu^{3+} coordination sphere) by the used organic ligands.

The CIE diagram (Fig. 5) shows the resulting emission color detected by the human eye. The high color purity is achieved due to the high relative intensity of the Eu^{3+} ion $^5D_0 \rightarrow {}^7F_2$ transition, that dominate the spectral profile, and the absence or low intensity of a band arisen from organic components of the materials.

4. Conclusion

In summary, it was demonstrate the feasibility of improving the luminescence emission of Eu@COK-16 by replacing the water molecules in the first coordination sphere of Eu^{3+} through the impregnation of the MOF crystals with organic ligands such as acetylacetonate (ACAC), butyl sulfoxide (Butyl) and dimethyl sulfoxide (DMSO). X-ray diffraction patterns show the preservation of the COK-16 structure in all the samples except for the ACAC. SEM images present the morphologies consistent with the X-ray results,*i.e.* it is possible to observe the initial intact COK-16 octahedral crystals deteriorating after the contact with the ACAC ligand. The behaviour of the luminescence profiles presented by the materials indicate the water/ligands substitution around the Eu^{3+}. In addition, the Judd-Ofelt parameters Ω_2 and Ω_4 suggest a less symmetrical chemical environment around the rare earth ion due to the presence of the coordinated ligands in the vicinity of the rare earth ion. Finally, by reducing the coordinate water content, it was observed an increase in the quantum efficiency for those systems.

Author statement

Prof. Dr. Danilo Mustafa designed the research plan, contributed to the interpretation of the results and prepared the manuscript. Dr. Ivan G. N. Silva contributed to the experimental design, synthesis and characterization of Eu@COK-16 and the impregnation with the organic ligands and assisted in the writing of the manuscript.

Fig. 5. CIE diagram for the Eu@COK-16 and impregnated with DMSO, Butyl, ACAC1, all materials have resulting colour contained inside the black circle [31].

Declaration of competing interest

The authors declare that they have no known competing financial interests or personal relationships that could have appeared to influence the work reported in this paper.

Acknowledgments

The authors acknowledge financial support from Fundação de Amparo à Pesquisa do Estado de São Paulo (FAPESP, 2011/19352-9 and 2015/19210-0), Conselho Nacional de Desenvolvimento Científico e Tecnológico (CNPq, 403055/2016-4) and Coordenação de Aperfeiçoamento de Pessoal de Nível Superior (CAPES, 88882.315485/2019–01).

References

[1] K. Binnemans, Interpretation of europium(III) spectra, Coord. Chem. Rev. 295 (2015) 1–45, https://doi.org/10.1016/j.ccr.2015.02.015.
[2] H.F. Brito, O.L. Malta, M.C.F.C. Felinto, E.E.S. Teotonio, Luminescence phenomena involving metal enolates, in: PATAI'S Chem. Funct. Groups, John Wiley & Sons, Ltd, Chichester, UK, 2010, p. 1210, https://doi.org/10.1002/9780470682531.pat0419.
[3] H.M. Carnall, W.T. Crosswhite, H. Crosswhite, Energy Level Structure and Transition Probabilities of the Trivalent Lanthanides in LaF_3, Argonne National Laboratory, U.S.A., 1978. http://www.osti.gov/scitech/biblio/6417825.
[4] I.G.N. Silva, L.C. V Rodrigues, E.R. Souza, J. Kai, M.C.F.C. Felinto, J. Hölsä, H. F. Brito, O.L. Malta, Low temperature synthesis and optical properties of the R_2O_3: Eu^{3+} nanophosphors (R^{3+}: Y, Gd and Lu) using TMA complexes as precursors, Opt. Mater. 40 (2015) 41–48, https://doi.org/10.1016/j.optmat.2014.11.044.
[5] P. Mahata, S.K. Mondal, D.K. Singha, P. Majee, Luminescent rare-earth-based MOFs as optical sensors, Dalton Trans. 46 (2017) 301–328, https://doi.org/10.1039/C6DT03419E.
[6] J.L. Wang, F.Y. Bai, Z. Wang, Z.Y. Deng, Y.H. Xing, Synthesis, crystal structures and luminescence of organic-lanthanide complexes with nicotinic acid and adipic acid ligands, J. Inorg. Organomet. Polym. Mater. 22 (2012) 807–815, https://doi.org/10.1007/s10904-011-9641-0.
[7] D. Mustafa, I.G.N. Silva, S.R. Bajpe, J.A. Martens, C.E.A. Kirschhock, E. Breynaert, H.F. Brito, Eu@COK-16, a host sensitized, hybrid luminescent metal–organic

framework, Dalton Trans. 43 (2014) 13480–13484, https://doi.org/10.1039/C4DT00899E.
[8] P.F. Smet, J. Botterman, K. Van Den Eeckhout, K. Korthout, D. Poelman, Persistent luminescence in nitride and oxynitride phosphors: a review, Opt. Mater. 36 (2014) 1913–1919, https://doi.org/10.1016/j.optmat.2014.05.026.
[9] R. Mani, H. Jiang, S.K. Gupta, Z. Li, X. Duan, Role of synthesis method on luminescence properties of europium(II, III) ions in β-Ca_2SiO_4: probing local site and structure, Inorg. Chem. 57 (2018) 935–950, https://doi.org/10.1021/acs.inorgchem.7b01878.
[10] T. Wu, P. Bouř, V. Andrushchenko, Europium (III) as a circularly polarized luminescence probe of DNA structure, Sci. Rep. 9 (2019) 3–7, https://doi.org/10.1038/s41598-018-37680-7.
[11] C.A. Destefani, L.C. Motta, R.A. Costa, C.J. Macrino, J.F.P. Bassane, J.F.A. Filho, E. M. Silva, S.J. Greco, M.T.W.D. Carneiro, D.C. Endringer, W. Romão, Evaluation of acute toxicity of europium-organic complex applied as a luminescent marker for the visual identification of gunshot residue, Microchem. J. 124 (2016) 195–200, https://doi.org/10.1016/j.microc.2015.08.021.
[12] I. Villa, C. Villa, A. Monguzzi, V. Babin, E. Tervoort, M. Nikl, M. Niederberger, Y. Torrente, A. Vedda, A. Lauria, Demonstration of cellular imaging by using luminescent and anti-cytotoxic europium-doped hafnia nanocrystals, Nanoscale 10 (2018) 7933–7940, https://doi.org/10.1039/c8nr00724a.
[13] H. Gallardo, H.C. Braga, P. Tuzimoto, A. Bortoluzzi, C.A.M. Salla, I.H. Bechtold, J. S. Martins, C. Legnani, W.G. Quirino, Synthesis, structure and OLED application of a new europium(III) complex: {tris-(thenoyltrifluoroacetonate)[1,2,5] selenadiazolo[3,4-f][1,10]phenanthroline}europium(III), Inorg. Chim. Acta. 473 (2018) 75–82, https://doi.org/10.1016/j.ica.2017.12.034.
[14] R. Reyes, M. Cremona, H.F. Brito, Room temperature molecular electrophosphorescence detection in organic LEDs with (Gd, Eu)-β-diketonate complexes blend, Opt. Mater. 84 (2018) 631–635, https://doi.org/10.1016/j.optmat.2018.07.062.
[15] T. Näreoja, J.M. Rosenholm, U. Lamminmäki, P.E. Hänninen, Super-sensitive time-resolved fluoroimmunoassay for thyroid-stimulating hormone utilizing europium (III) nanoparticle labels achieved by protein corona stabilization, short binding time, and serum preprocessing, Anal. Bioanal. Chem. 409 (2017) 3407–3416, https://doi.org/10.1007/s00216-017-0284-z.
[16] J. Xu, K. Haupt, B.T.S. Bui, Core-shell molecularly imprinted polymer nanoparticles as synthetic antibodies in a sandwich fluoroimmunoassay for trypsin determination in human serum, ACS Appl. Mater. Interfaces 9 (2017) 24476–24483, https://doi.org/10.1021/acsami.7b05844.
[17] J.L. Kropp, M.W. Windsor, Luminescence and energy transfer in solutions of rare-earth complexes. I. Enhancement of fluorescence by deuterium substitution, J. Chem. Phys. 42 (1965) 1599–1608, https://doi.org/10.1063/1.1696166.
[18] S.R. Bajpe, E. Breynaert, A. Martin-Calvo, D. Mustafa, S. Calero, C.E.A. Kirschhock, J.A. Martens, COK-16: a cation-exchanging metal-organic framework hybrid, Chempluschem 78 (2013) 402–406, https://doi.org/10.1002/cplu.201300080.
[19] D. Maffeo, J.A.G. Williams, Intramolecular sensitisation of europium(III) luminescence by 8-benzyloxyquinoline in aqueous solution, Inorg. Chim. Acta. 355 (2003) 127–136, https://doi.org/10.1016/S0020-1693(03)00338-4.
[20] I.G.N. Silva, D. Mustafa, B. Andreoli, M.C.F.C. Felinto, O.L. Malta, H.F. Brito, Highly luminescent Eu^{3+}-doped benzenetricarboxylate based materials, J. Lumin. 170 (2016) 364–368, https://doi.org/10.1016/j.jlumin.2015.04.047.
[21] I.G.N. Silva, J. Kai, M.C.F.C. Felinto, H.F. Brito, White emission phosphors based on Dy^{3+}-doped into anhydrous rare-earth benzenetricarboxylate complexes, Opt. Mater. 35 (2013) 978–982, https://doi.org/10.1016/j.optmat.2012.12.001.
[22] L.A. Bueno, A.S. Gouveia-Neto, E.B. Costa, Y. Messaddeq, S.J.L. Ribeiro, Structural and spectroscopic study of oxyfluoride glasses and glass-ceramics using europium ion as a structural probe, J. Phys. Condens. Matter 20 (2008), https://doi.org/10.1088/0953-8984/20/14/145201.
[23] J.C.G. Bünzli, Lanthanide luminescence for biomedical analyses and imaging, Chem. Rev. 110 (2010) 2729–2755, https://doi.org/10.1021/cr900362e.
[24] A. Zaïm, S.V. Eliseeva, L. Guénée, H. Nozary, S. Petoud, C. Piguet, Lanthanide-to-lanthanide energy-transfer processes operating in discrete polynuclear complexes: can trivalent europium be used as a local structural probe? Chem. Eur J. 20 (2014) 12172–12182, https://doi.org/10.1002/chem.201403206.
[25] I.G.N. Silva, C.S. Cunha, A.F. Morais, H.F. Brito, D. Mustafa, Eu^{3+} or Sm^{3+}-Doped terbium-trimesic acid MOFs: highly efficient energy transfer anhydrous luminophors, Opt. Mater. 84 (2018) 123–129, https://doi.org/10.1016/j.optmat.2018.06.065.
[26] O.L. Malta, P.A. Santa-Cruz, G.F. De Sá, F. Auzel, Time evolution of the decay of the $^5D_0$ level of Eu^{3+} in glass materials doped with small silver particles, Chem. Phys. Lett. 116 (1985) 396–399, https://doi.org/10.1016/0009-2614(85)80191-3.
[27] Z. Wang, Y.-H. Xing, C.-G. Wang, L.-X. Sun, J. Zhang, M.-F. Ge, S.-Y. Niu, Synthesis, structure and luminescent properties of coordination polymers with 1,2-benzene-dicarboxylic acid and a series of flexible dicarboxylate ligands, CrystEngComm 12 (2010) 762–773, https://doi.org/10.1039/B916127A.
[28] I.G.N. Silva, D. Mustafa, M.C.F.C. Felinto, W.M. Faustino, E.E.S. Teotonio, O. L. Malta, H.F. Brito, Low temperature synthesis of luminescent RE_2O_3:Eu^{3+} nanomaterials using trimellitic acid precursors, J. Braz. Chem. Soc. 26 (2015) 2629–2639, https://doi.org/10.5935/0103-5053.20150314.
[29] K. Binnemans, K. Van Herck, C. Görller-Walrand, Influence of dipicolinate ligands on the spectroscopic properties of europium(III) in solution, Chem. Phys. Lett. 266 (1997) 297–302, https://doi.org/10.1016/S0009-2614(97)00012-2.
[30] I.G.N. Silva, A.F. Morais, D. Mustafa, Synthesis, characterization and Judd-Ofelt analysis of Sm^{3+}-doped anhydrous Yttrium trimesate MOFs and their Y_2O_3:Sm^{3+} low temperature calcination products, J. Lumin. 210 (2019) 335–341, https://doi.org/10.1016/j.jlumin.2019.02.048.
[31] P.A. Santa-Cruz, F.S. Teles, Spectra Lux Software v.2.0 Beta, Ponto Quântico Nanodispositivos, RENAMI, 2003.